

Expanded View Figures

Figure EV1. Active RET leads to increased ROS and decreased NAD⁺/NADH ratio in aged flies.

- A, B Mito-Sox staining (A) and data quantification (B) showing mitochondrial ROS level in different aged fly brains with or without treatment with the indicated RET inhibitors ($n = 5$ per group).
- C Quantification of NAD⁺/NADH ratio in young flies, old flies, and old flies treated with the indicated chemicals.
- D Western blot analysis comparing NDUFS3 level in young and aged flies. $**P < 0.01$ in Student's t -test.
- E Quantification of FET-ROS in isolated mitochondria purified from aged wild-type flies and assayed under FET condition without or with treatment at the indicated concentrations of CPT ($n = 4$).
- F Quantification of NAD⁺/NADH ratio in isolated mitochondria after induction of FET and with or without CPT (2.5 μ M) treatment ($n = 4$).
- G Co-immunoprecipitation assay showing the effect of aging and CPT treatment on the various protein–protein interactions between C-I proteins involved in RET.
- H Quantification of ROS level from brain samples of DES and DES + CPT-treated flies ($n = 4$).
- I Quantification of NAD⁺/NADH ratio from brain samples of DES and DES + CPT-treated flies ($n = 5$ sets, 20 flies per set).
- J Quantification of NAD⁺ and NADH levels measured with SoNar in different aged fly brains with or without treatment with the indicated chemicals as shown in Fig 1D ($n = 4$ sets, 5 flies per set).
- K Quantification of NAD⁺/NADH ratio in wild-type flies treated with CPT or co-treated with CPT and NADH ($n = 4$ sets, 20 flies per set).
- L Mitochondrial C-I activity assay using mitochondria purified from different aged flies ($n = 3$).
- M In-gel activity assays of respiratory complexes using mitochondria purified from different aged flies.

Data information: Data are representative of at least three repeats. Data are shown as mean \pm SEM. Asterisks indicate statistical significance ($**P < 0.01$) in single-factor ANOVA with Scheffe's analysis as a *post hoc* test.

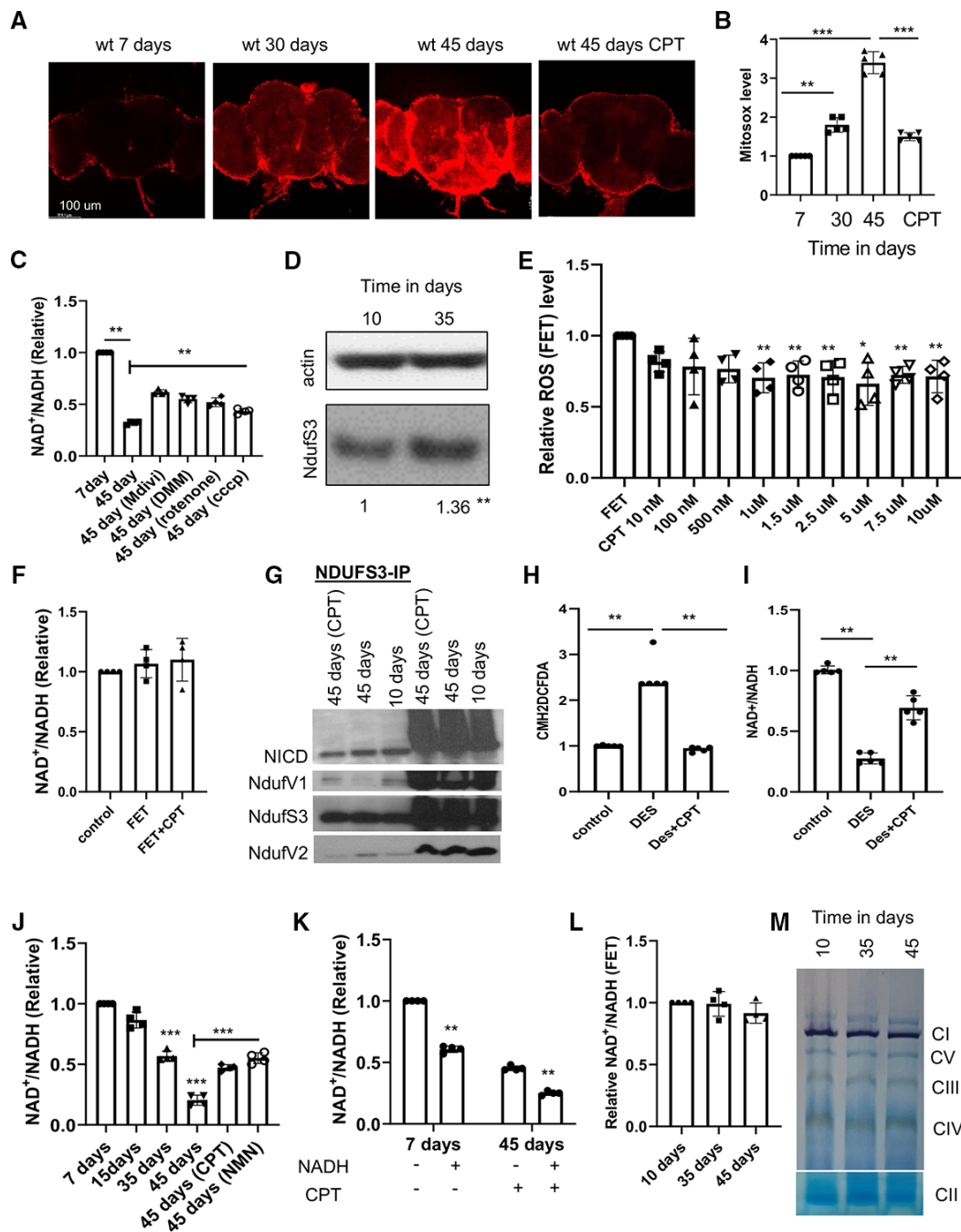


Figure EV1.

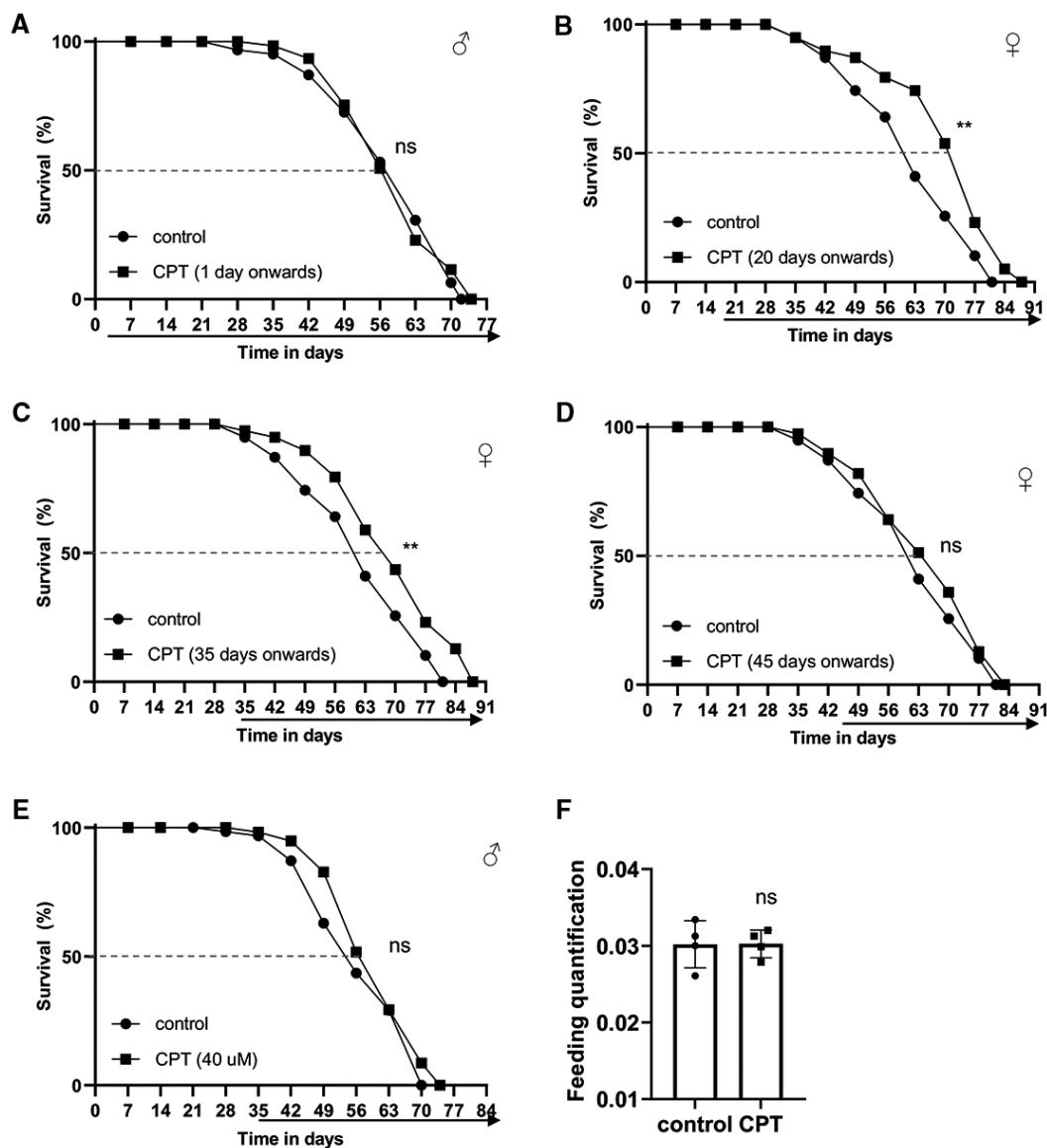


Figure EV2. Inhibition of RET by CPT treatment extends *Drosophila* lifespan.

A Survival curves comparing control flies and flies fed with food containing 10 μ M CPT from day 1 onwards.

B–D Survival curves comparing overall survival (by logrank test) and maximum lifespan (by Wang–Allison test) of control flies and flies fed with food containing 10 μ M CPT from 20 days (** $P < 0.001$ logrank, ** $P < 0.001$ Wang–Allison) (B), 35 days (** $P < 0.001$ logrank, ** $P < 0.001$ Wang–Allison) (C), and 45 days (ns) (D) onwards ($n = 3$ groups, 20–25 flies per group).

E Survival curves comparing control flies and flies fed with food containing 40 μ M CPT from 35 days onwards (ns; $n = 3$ groups, 20–25 flies per group).

F Quantification of food consumption in control and CPT-fed flies ($n = 4$ groups, 20 per group).

Data information: Data are representative of at least three repeats. Data are shown as mean \pm SEM in (F). Survival curves were analyzed with logrank test along with Wang–Allison test for maximum lifespan. Dashed lines mark time points of 50% survival. Asterisks indicate statistical significance (** $P < 0.01$, ns: not significant) in single-factor ANOVA with Scheffé's analysis as a *post hoc* test.

Figure EV3. Inhibition of RET by genetic manipulation of C-I subunits extends fly lifespan.

- A, B Survival curves of control flies and flies with NDUFS2 (A), or NDUFS3 (B) knocked down in neurons ($n = 3$ groups, 20–25 flies per group).
- C Quantification of food consumption in flies treated with CPT or NMN.
- D Quantification of Smurf assay data in young flies, old flies, and old flies treated with CPT and NMN ($n = 3$ groups, 20 flies per group).
- E–I Survival curves showing the lifespan effect of CPT in combination with NMN (E) (control vs NMN: $**P < 0.01$ logrank, $**P < 0.01$ Wang Allison; CPT vs CPT + NMN, ns), mito-Tempo (F) (control vs mito-Tempo: $**P < 0.01$ logrank, $**P < 0.01$ Wang Allison; CPT vs CPT + mito-Tempo: ns), melatonin (G) (control vs melatonin: $**P < 0.01$ logrank, $**P < 0.01$ Wang Allison; CPT vs CPT+ melatonin: ns), FK866 (H) (control vs FK866: $**P < 0.01$ logrank, $**P < 0.01$ Wang Allison; FK866 vs FK866 + CPT: ns), and paraquat (I) (control vs paraquat: $**P < 0.01$ logrank, $**P < 0.01$ Wang Allison; paraquat vs paraquat+CPT: ns) ($n = 3$ groups, 20 flies per group).

Data information: Data are representative of at least three repeats. Data are shown as mean \pm SEM in (C, D). Survival curves were analyzed with logrank test along with Wang–Allison test for maximum lifespan. Dashed lines mark time points of 50% survival. Asterisks indicate statistical significance ($**P < 0.01$) in single-factor ANOVA with Scheffe's analysis as a *post hoc* test.

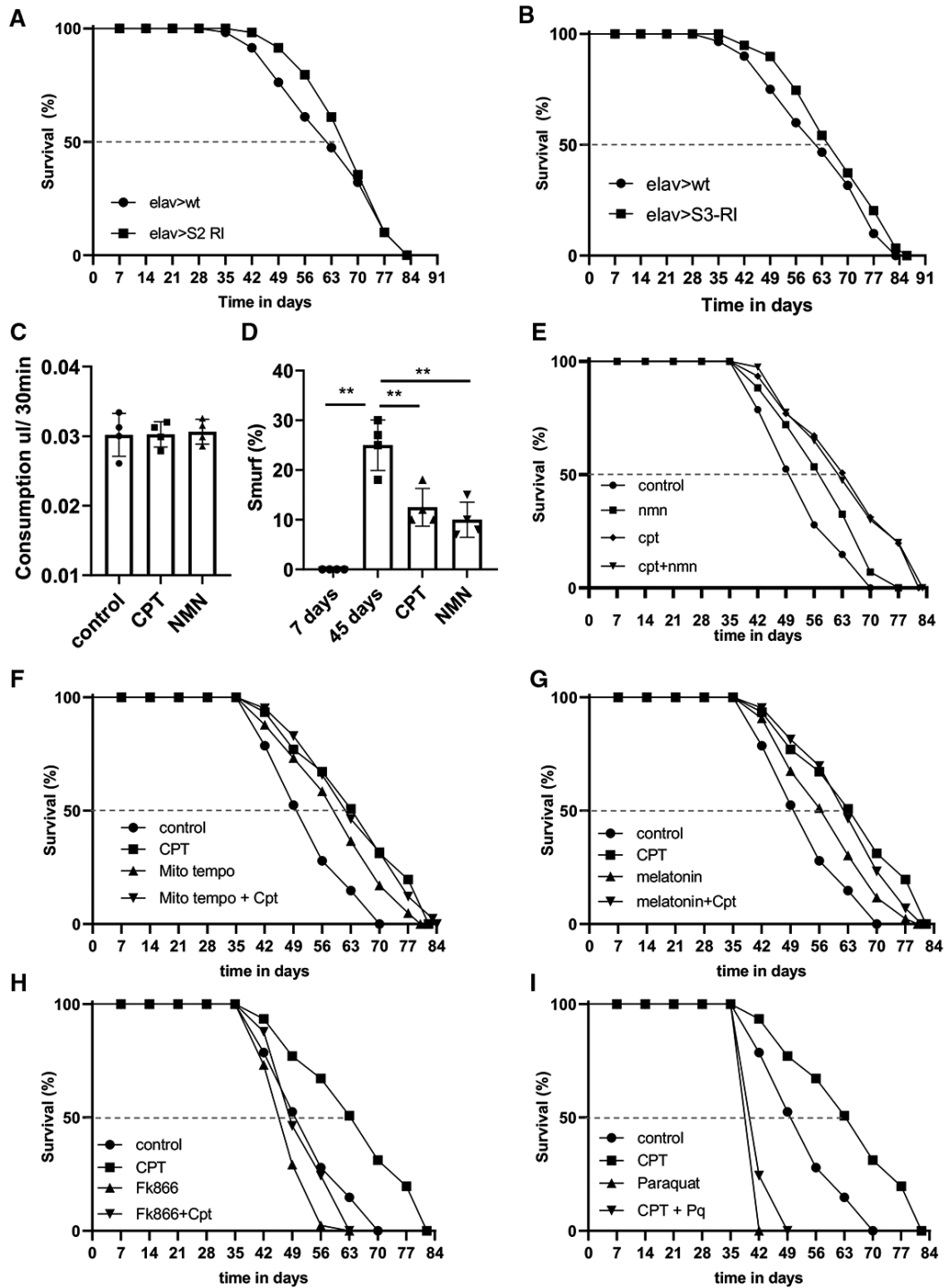


Figure EV3.

Figure EV4. Lifespan effect of RET inhibition by CPT is mediated by Sirtuin, Foxo, and autophagy pathways.

- A, B Immunoblots showing the effect of aging on dFoxo acetylation (A), and effect of CPT treatment on dFoxo acetylation (B). dFoxo was immunoprecipitated from whole fly extracts and detected with anti-acetyl-K antibody.
- C RT-PCR analysis of levels of the indicated transcripts in aged flies relative to young flies.
- D Images and data quantification showing p62 staining in the brain of old flies and old flies treated with CPT ($n = 5$ per group).
- E–I Survival curve showing the effect of NMN on lifespan in control (*Mhc > wt*) flies (** $P < 0.01$, logrank) (E), and NDUFS3-RNAi (F), Foxo-RNAi (** $P < 0.01$, logrank) (G), Sirt-2-RNAi (H), and ATG1-RNAi (** $P < 0.01$, logrank) (I) flies ($n = 3$ groups, 20 flies per group).

Data information: Data are representative of at least three repeats. Data are shown as mean \pm SEM in (C, D). Survival curves were analyzed with logrank test along with Wang–Allison test for maximum lifespan. Dashed lines mark time points of 50% survival. Asterisks indicate statistical significance (*** $P < 0.001$, ** $P < 0.01$, * $P < 0.05$) in single-factor ANOVA with Scheffe's analysis as a *post hoc* test.

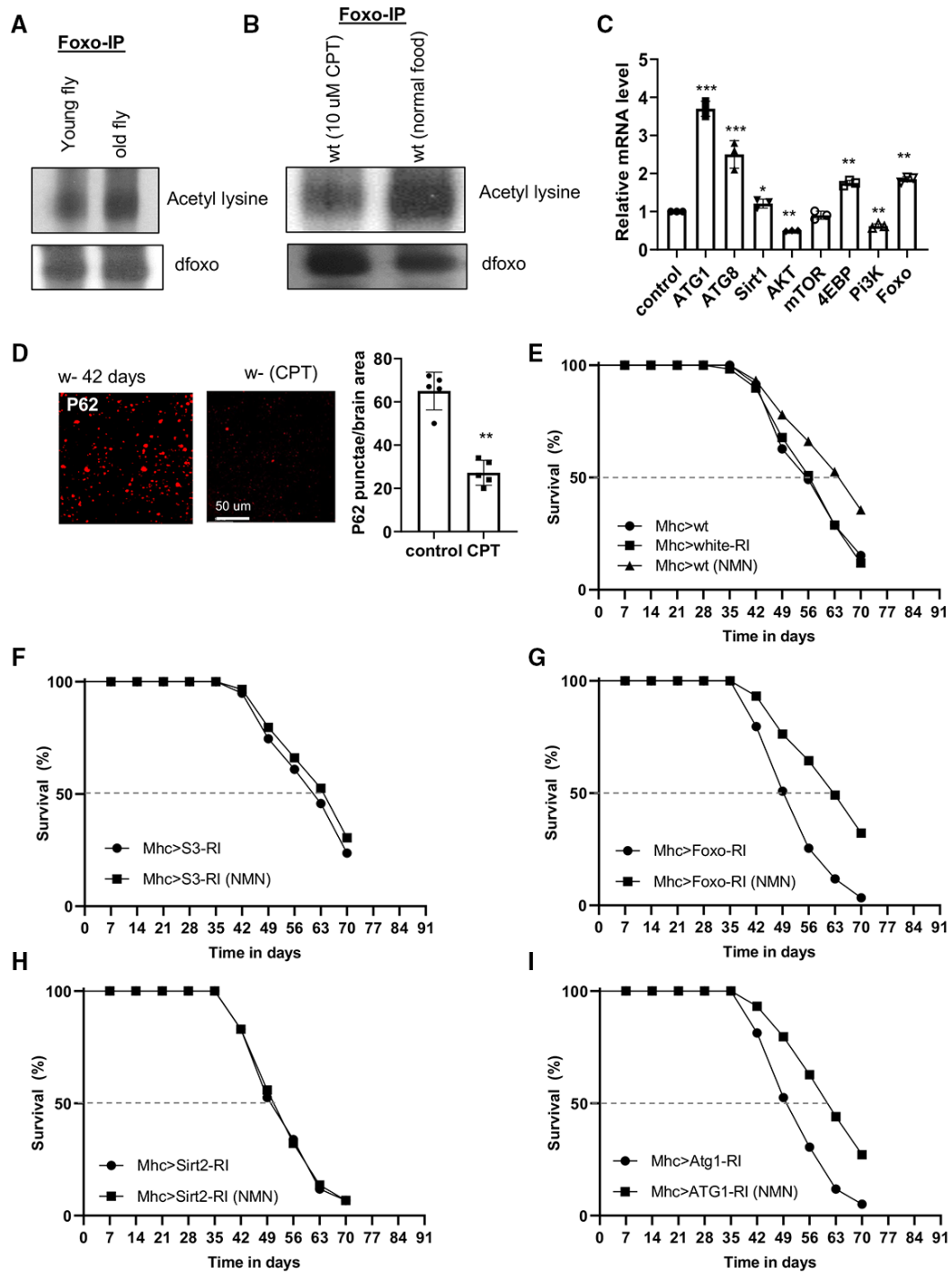


Figure EV4.

Figure EV5. Inhibition of RET rescues disease phenotypes of fly AD models.

- A Staining images and data quantification showing the effect of CPT on ROS level in the brain of *elav > APP.BACE* flies ($n = 3$ set, 5 brains per set).
- B Immunofluorescence images and data quantification showing the effect of CPT on mitochondrial morphology in DA neurons of *TH > APP.C99* flies co-expressing a mito-GFP reporter ($n = 5$ brains per group).
- C Immunofluorescence images showing the effect of CPT treatment on lysosomal morphology in the muscle of *Mhc > APP.C99* flies.
- D Immunofluorescence images showing the effect of CPT treatment on DA neuron number in the PPL1 cluster of *elav > APP.BACE* fly brain.
- E, F Immunostaining showing the effect of NDUFS3-RNAi on 6E10-positive amyloid (E) and ubiquitin- and p62-positive protein aggregates (F) in the muscle of *Mhc > APP.C99* flies.
- G Quantification of the effect of AOX or NMNAT overexpression on wing posture in *Mhc > APP.C99* flies ($n = 4$ groups, 20 flies per group).
- H Immunoblots showing the effect of AOX or NMNAT overexpression on aberrant APP.C99 translation products in *Mhc > APP.C99* flies.
- I Quantification of the effect of dFoxo overexpression on wing posture in *Mhc > APP.C99* flies ($n = 4$ groups, 20 flies per group).

Data information: Data are representative of at least three repeats. Data are shown as mean \pm SEM. Asterisks indicate statistical significance (** $P < 0.001$, ** $P < 0.01$) using single-factor ANOVA with Scheffe's analysis as a *post hoc* test.

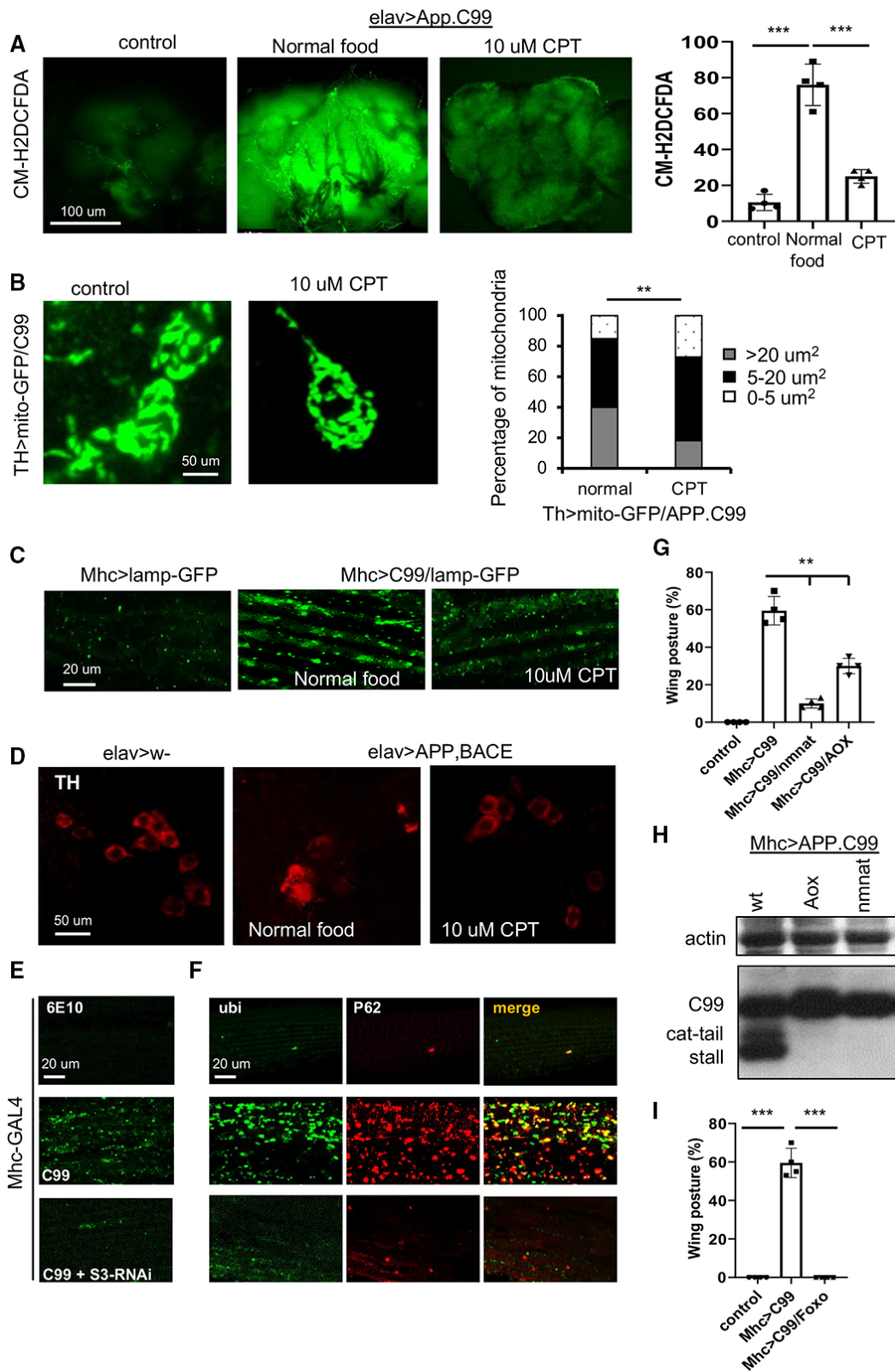


Figure EV5.